Windmill Palm (*Trachycarpus fortunei*) Fibers for the Preparation of Activated Carbon Fibers

Chao Li,[a] Jian Lin,[a,*] Guangjie Zhao,[a,*] and Jianhui Zhang [b]

Activated carbon fibers (ACFs) were prepared by steam activation of windmill palm (WP) (*Trachycarpus fortunei*) fibers in a nitrogen atmosphere at various temperatures in the 600 to 850 °C range, and their characteristics were investigated. The effects of temperature, in terms of porous texture and surface chemistry, were identified through the use of scanning electron microscopy (SEM), nitrogen adsorption-desorption, mercury intrusion porosimetry (MIP), X-ray photoelectron spectroscopy (XPS), and Fourier transform infrared (FTIR) spectroscopy. The results showed that the ACFs prepared at relatively high temperatures presented more cracking, collapsed surfaces, and lower yields because of the violent reaction that occurred during the activation process. With increasing temperature, more micropores were generated, and then the number eventually declined because of the conversion of partial micropores into mesopores. The ACFs with the highest special surface area, 1320 m^2/g, and total pore volume, 1.416 cm^3/g, were obtained at the activation temperature of 850 °C. In addition, graphitic carbon, the main compound on the surface of ACFs, decreased. Conversely, the amount of functional groups containing C-O (except for C-OH) slightly increased with increasing activation temperatures. It was also found that the mesopore volume and methylene blue adsorption of ACFs were highly increased as the temperature increased from 600 to 850 °C. Accordingly, WP fibers are a promising precursor for ACF production.

Keywords: Windmill palm fiber; Activation; Activated carbon fibers; Pore structure

Contact information: a: MOE Key Laboratory of Wooden Material Science and Application, Beijing Forestry University, Beijing, 100083, P. R. China; b: Planning and Design Institute of Forest Products Industry, SFA, Beijing, 100010, P. R. China;
** Corresponding authors: linjian0702@bjfu.edu.cn; zhaows@bjfu.edu.cn*

INTRODUCTION

Activated carbon fibers (ACFs) are one kind of promising carbon nanoporous materials with fiber shapes and well-defined porous structures, produced by the pyrolysis of carbonaceous materials followed by an additional activation process (Lee *et al*. 2014). Nowadays, ACFs have been more widely applied because of their unique characteristics. For example, the large surface areas of ACFs facilitate their performance as adsorbents. High porosity is extremely desirable for enhanced performance of adsorbents since it facilitates high mass transfer fluxes and catalyst/adsorbate loading. Also, the tailored porosity and pore size distribution have widened the usefulness of ACFs to more demanding applications, such as separation of multi-sized molecules, electronic materials, catalyst supports, and the storage of natural gas (Suzuki 1994; Jain *et al*. 2016). In general, ACFs are commercially manufactured from precursors such as pitch, polyacrylonitrile, viscose rayon, and phenolic resin with the procedures of spinning, thermostabilization, carbonization, and activation. However, such petrochemical precursors are costly and not

environmentally friendly, because of the decreasing reserves of fossil fuels and resultant negative effects of their use in terms of generation of greenhouse gases and acid rain. Recently, natural fibers have received increasing attention as low-cost and renewable precursors for preparing ACFs.

Biomass is a good alternative for replacing petrochemical precursors because of its abundance and sustainability. There have been many studies concentrated on preparing ACFs or adsorbents from biomass such as sisal (Chen and Zeng 2003), hemp (Rosas *et al*. 2009; Yang *et al*. 2011), cotton (Zheng *et al*. 2014), bamboo (Zhao *et al*. 2015), silkworm cocoon (Li *et al*. 2015), and wood (Liu *et al*. 2014). One important natural resource, windmill palm (WP) fibers, comprise rigid fibers extracted from leaves of the palm tree (*Trachycarpus fortunei*), which have been growing naturally in China for centuries. Normally, the primary use of the WP fibers is in the production of domestic compliant materials such as mattresses, ropes, and coverings (Zhai *et al*. 2012). Moreover, the amount of Klason lignin found in these fibers (nearly 40%) is large in comparison to other lignocellulosic materials. In addition, the ash level (0.2%) is relatively low (Zhai *et al*. 2013), which provides a favorable substitution for carbon material precursors (Suhas and Carrott 2007). These characteristics of the WP fibers are quite favorable for their use in the production of ACFs.

Generally, there are two basic processes to activate carbon materials: physical and chemical. Chemical activation can be accomplished by carrying out thermal decomposition of raw material with chemical reagents. Zhang *et al*. (2008), for example, prepared ACF from WP tegument by biochemical method using bio-fermentation technology and phosphoric acid as activating agents. In contrast, physical activation, especially steam activation, is a zero effluent discharge process with no addition of solid or liquid chemicals. Steam activation conforms to the need for cleaner and low cost production, and the product can be widely used in many fields, such as in pharmaceutical and food industries. Therefore, in production, steam activation is more favorable than chemical activation. However, no report used steam as an activating agent, and no report has yet been published on the influence of activation parameters on the characteristics of WP fiber-based ACF produced by steam activation.

Accordingly, in this work, the utilization of WP fibers as a raw material for the preparation of ACFs using a steam activation process, and the characterization of the materials was completed using technical methods. The adsorption characteristics of the obtained samples in the liquid phase were also investigated, where methylene blue (MB) was used as a representative adsorbate.

EXPERIMENTAL

Preparation of ACFs

The WP fibers used in this study were produced at Yunnan Province in China. The biochemical composition analyses of the WP fibers were measured as 41.1, 23.1, and 34.7, 0.6 and 0.2 % for cellulose, hemicellulose, lignin, extractives and ash on dry basis, respectively. The average ultimate analyses were 48.1, 5.9, 45.6, and 0.4 % for C, H, O, and N contents, respectively. The bulk density was 0.73 g/cm^3. The fibers were cleaned from leaf sheaths and then air dried for several days. Next, the fibers were placed into a tube furnace (Manufactured by Beijing Forestry University) and carbonized for 1 h under an N_2 atmosphere. The activation was conducted in the same furnace, and the carbonized

samples were heated from room temperature to the final activation temperature with a heating rate of 4 °C/min under an N_2 flow rate of 200 cm^3/min. Thereafter, the fibers were isothermally heated for 1 h with a steam flow rate of 3.1 mL/min and then cooled to room temperature. The activation temperatures were the same as the carbonization temperatures: 600, 700, 800, and 850 °C, respectively. The samples are referred to as ACFs-600, ACFs-700, ACFs-800, and ACFs-850, respectively. The yield was calculated as the weight ratio of ACFs to WP fibers.

Characterization

Scanning electronic microscopy (SEM)

The surface morphology of the WP fibers and ACFs were examined using scanning electron microscopy (SEM; S-3400N, Hitachi Co. Ltd., Chiyoda, Tokyo, Japan) at magnifications of 200 to 1,200 X and at an accelerating voltage of 5 kV. Before observation, the samples were coated with a thin layer by spraying gold metal using Ion Sputter (E-1010, Hitachi Co. Ltd., Chiyoda, Tokyo, Japan) before searching morphology.

Porous structure

The textural parameters of the ACFs were determined using N_2 adsorption-desorption isotherms at 77 K (Autosorb-iQ, Quantachrome Instruments Japan GK, Kanagawa, Japan). In preparation, the ACFs were degassed at 300 °C for 3 h. The specific surface area (S_{BET}) was calculated by the Brunauer-Emmett-Teller (BET) method using N_2 adsorption isotherm data. The total pore volume (V_{tot}) was evaluated by converting the amount of N_2 adsorbed at a relative pressure of 0.995 to the volume of liquid adsorbate. The micropore area (S_{micro}) and micropore volume (V_{micro}) were obtained by the t-plot method. The mesopore area (S_{meso}) and mesopore volume (V_{meso}) were calculated according to the Barrett-Joyner-Halenda (BJH) method. The pore size distribution (PSD) was calculated using the density functional theory (DFT) method (Lastoskie *et al.* 1993), which is based on the calculated N_2 adsorption isotherms for different pore sizes.

Mercury intrusion porosimetry (MIP)

The pore structures of WP fibers were characterized using mercury porosimetry (AutoPore IV 9500, Micromeritics, Norcross, GA, USA), in the pressure range of 0.2 to 44,500 psi and an equilibration time of 10 s (Leon 1998).

Fourier transform infrared spectroscopy

The chemical groups of the WP fibers and ACFs were examined using Fourier transform infrared (FTIR) spectrum analysis with a spectrometer (Tensor 27, Bruker Optics, Ettlingen, Germany), in the scanning range of 4000 to 400 cm^{-1}. The samples were pulverized using size 100 mesh and mixed with potassium bromide at the ratio of 1:100, before being pressed into a disk.

X-ray photoelectron spectroscopy

X-ray photoelectron spectroscopy (XPS) measurements were carried out on a spectrophotometer (ESCALAB 250Xi, Thermo Fisher Scientific Inc., Waltham, MA, USA) to determine the number of functional groups present on the surface of the WP fibers/ACFs with a monochromated Al Ka X-ray source (hv = 1486.6 eV). A current of 10 mA and a voltage of 13 kV were used. The survey scans were collected from the binding energy range of 0 to 1350 eV. A nonlinear, least squares regression analysis program

(XPSPEAK software, Version 4.1., Informer Technologies, Inc., Hong Kong, China) was used for the XPS spectral deconvolution.

Adsorption methods of methylene blue *(MB)*

The methylene blue (MB, CAS 7220-79-3, Tianjin Jinke Fine Chemicals CO. Ltd, China) removal was obtained from an adsorption test where 0.1 g of ACF was added to a 150 mL flask containing 50 mL of an MB solution with an initial concentration of 300 mg/L and shaken at 240 rpm for 1 h at room temperature (25 °C). The final MB concentration was determined using a UV-vis spectroscopy (Bioware II, WPA, England) by measuring the light absorbance at a wavelength of 665 nm.

RESULTS AND DISCUSSION

Yield and Morphologies of ACFs

Generally, an efficient ACF production process combines a well-developed porosity with an acceptable fabrication yield. In the present study, the ACFs production yields were monitored for the four used activating temperatures. The yield percentages obtained for the ACFs prepared from WP fibers are shown in Table 1. The yield decreased from 27% to 1% with increasing activation temperature. However, there needed to be a compromise between properties and yield, and that perhaps 800 °C represented the upper limit of feasibility in the ACFs production, with the yield of 11%. This tendency was consistent with the results from the preparation of activated carbon from several agricultural wastes, such as bamboo, plum kernels, and corn cobs, in previous studies (Wu 1999a,b). The decrease in yield was caused by the reaction of steam with carbon, and a higher steam activation led to a higher burn off. What more, the burn-off higher than 50% in the case of steam activation always led to a development of mesoporosity due to the burning of the wall of micropore. Therefore, more porous structures were formed in ACFs, which could be observed from the SEM morphologies.

Table 1. Yield, N_2 Adsorption Properties, and the adsorption capacity for MB of WP Fibers and ACFs

Samples	Yield (%)	S_{BET} (m^2/g)	S_{micro} (m^2/g)	S_{meso} (m^2/g)	V_{tot} (cm^3/g)	V_{micro} (cm^3/g)	V_{meso} (cm^3/g)	MP-ratio[a] (%)	D[b] (nm)	MB adsorption (mg/g)
WP fibers	100	12	-	15	0.020	-	0.023	115.0	6.6	5
ACFs-600	27	501	345	127	0.317	0.142	0.155	48.9	2.5	177
ACFs-700	23	752	563	155	0.452	0.231	0.201	44.5	2.4	232
ACFs-800	11	1292	736	466	0.973	0.316	0.601	61.8	3.0	797
ACFs-850	1	1320	581	683	1.416	0.250	1.095	77.3	4.3	882

[a] The ratio of the mesopore volume to the total pore volume
[b] The average pore diameter

The SEM morphologies of the WP fibers and of the prepared ACFs are presented in Fig. 1. As shown in parts (a) and (b), the WP fibers have a cylindrical shape on the cross-section, distributed with a pattern of macropores, reflecting a considerably rough surface. After the carbonization and activation treatments, the morphology of the WP fibers was modified. Similar carbon structures with more uneven surfaces were presented. As shown in parts (c) through (j), as the temperature increased, more highly cracked and collapsed surfaces were obtained. Observation of the cross-sections exhibited honey-comb patterns

consisting of a lattice of adjacent cavities, similar to a very organized network of macropores. These textures are beneficial for any adsorption process, as wide pores serve as better channels when compared with pores of a smaller dimension (Zabaniotou *et al*. 2008). Therefore, more porous structures were created by increasing the activation temperature, which can be confirmed by N_2 adsorption and desorption measurements.

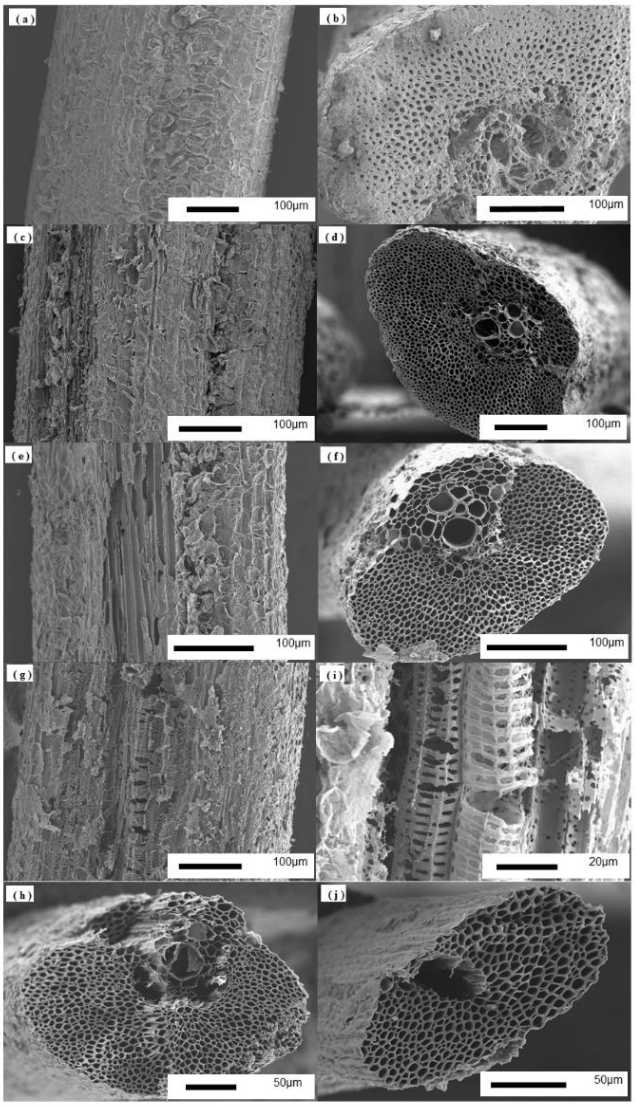

Fig. 1. SEM morphologies of WP fibers and of the prepared ACFs activated at various temperatures: (a) and (b) WP fibers; (c) and (d) 600 °C; (e) and (f) 700 °C; (g) and (h) 800 °C; (i) and (j) 850 °C

Characterization of Pore Structure

The isotherms of N_2 adsorption-desorption at 77 K of the WP fibers and ACFs are shown in Fig. 2. Compared with the ACFs, WP fibers absorbed a very small volume of N_2. Figure 2 shows that the uptake of N_2 linearly increased when the pressure was greater than 0.5 psi, implying that the WP fibers possibly had few micropores and a large number of mesopores and macropores. This was confirmed using MIP; mostly macropores (greater than 50 nm), a small number of mesopores (2 to 50 nm), and no micropores were observed (Fig. 3a).

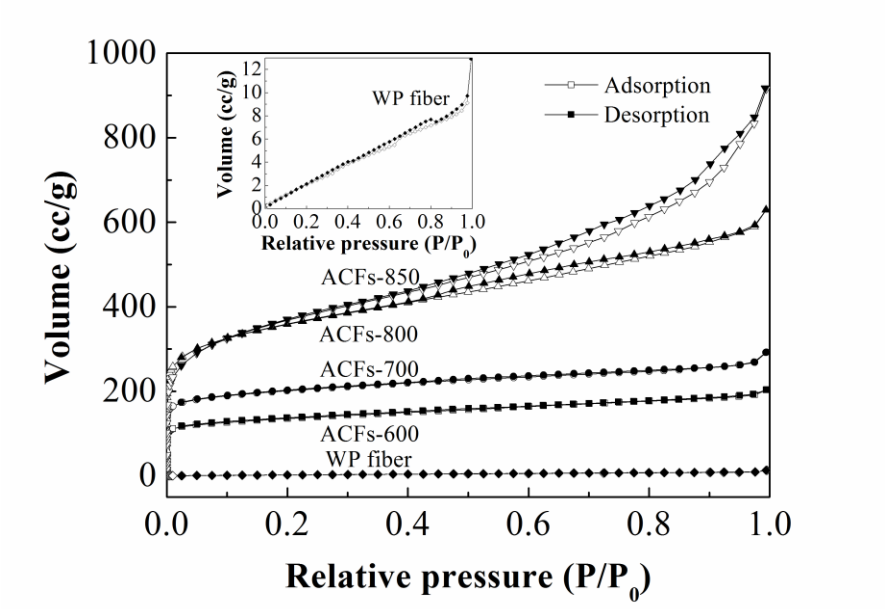

Fig. 2. N_2 adsorption-desorption isotherms at 77 K of WP fibers and ACFs

After the carbonization and activation treatments, both the ACFs-600 and ACFs-700 exhibited a type I isotherm, according to the International Union of Pure and Applied Chemistry (IUPAC) classification (Qian *et al*. 2007). Their major uptake occurred at a low relative pressure ($P/P_o < 0.05$) and reached a plateau as the relative pressure increased. This indicated that the activated carbon fibers were microporous. Different from ACFs-600 and ACFs-700, the isotherms of ACFs-800 had an open knee, and the slope of the plateau exhibited hysteresis loops at relative pressures of 0.4 to 0.8 because of multilayer adsorption, suggesting the coexistence of large micropores and mesopores. In the case of ACFs-850, wider open knees and larger hysteresis loops were obtained, indicating the co-existence of micropores and a considerable amount of large mesopores. In addition, the isotherms could also be analyzed in terms of their hysteresis loops type (Sing *et al*. 1985). According to the IUPAC standard classification, the style of hysteresis loops found for the ACFs produced by physical activation belonged to Type H3, which was observed in the case of aggregates of plate-like particles giving rise to slit-shaped pores (Ma *et al.* 2014).

The pore characteristics of WP fibers and ACFs are listed in Table 1. With increasing temperature, the S_{BET} and V_{tot} of ACFs gradually increased, and a considerable increase was observed after 700 °C. The S_{BET} and V_{tot} of ACFs-850 had maximum values of 1320 m^2/g and 1.416 cm^3/g, respectively. It is well known that reaction of carbon with steam is thermodynamically endothermic (Wigmans 1989) and the mechanism can be expressed as

$$C + H_2O \leftrightarrow C(H_2O) \quad (1)$$

$$C(H_2O) \rightarrow H_2 + C(O) \quad (2)$$

$$C(O) \rightarrow CO \quad (3)$$

$$C + H_2O \rightarrow CO + H_2 \quad \Delta H = +117 \text{ kJ mol}^{-1} \quad (4)$$

This observed increase in S_{BET} and V_{tot} of ACFs indicated that more violent reactions between steam and active amorphous atoms or unsaturated carbon atoms occurred during activation, forming numerous pores, gaps, and cracks as the temperature

rose, thus increasing the specific surface area and pore volume in weight (Liu and Zhao 2012; Su *et al*. 2012).

However, the dependences of V_{micro} and V_{meso} on the temperature in ACFs varied. The V_{meso} increased greatly as the temperature was increased from 600 to 850 °C. This suggested that a high activation temperature could promote the formation of mesopores, which can be attributed to larger original pore size and a smaller crystallite shape in the precursor fiber carbonization stage, aiding in the removal of carbon and the formation of larger pores (Jin and Zhao 2014). In contrast, the V_{micro} tended to decrease after 800 °C. And it should be noted that the S_{BET} kept increased after 800 °C. This suggested that part of existing micropores were widened into mesopores, and new micropores were regenerated, leading to the increase of S_{BET}. As a result, the MP ratio (the ratio of the mesopore volume to the total pore volume) increased with increasing temperature. At 850 °C, the composition of mesopores became dominant in the total pore volume, and the MP ratio reached 77.3%.

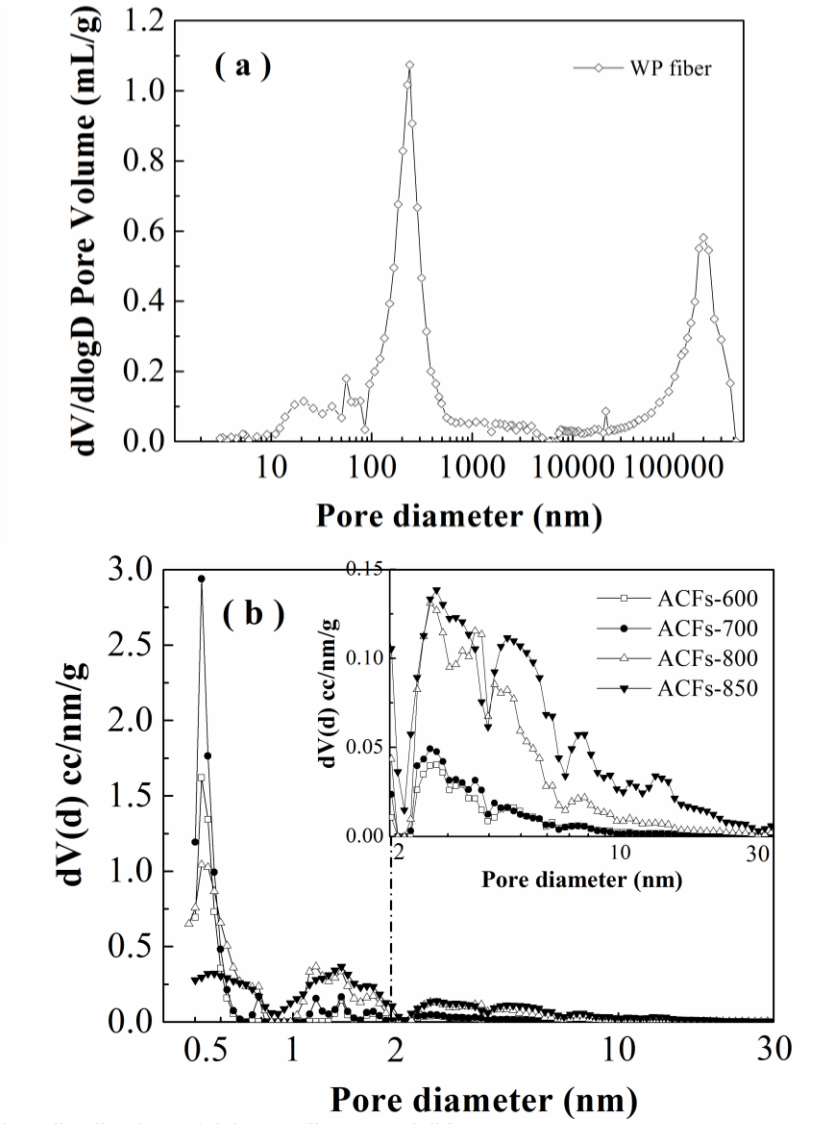

Fig. 3. Pore size distribution of (a) WP fibers and (b) ACFs

Details on the porosity of the ACFs produced are presented in Fig. 3(b). Obviously, ACFs obtained at lower temperatures (600 and 700 °C) exhibited narrow pore size distributions, with a pore width of 0.5 to 0.7 nm and 1.0 to 2.0 nm, respectively, which were assigned as micropores. At higher temperatures (800 and 850 °C), ACFs exhibited a wider range in pore sizes, from 0.5 to 10 nm, including both micropores and mesopores. In addition, as the temperature increased, the mainly micropore width was widened from 0.5 to 1.4 nm, and the mainly mesopore width was widened from 2.8 to 4.6 nm. Moreover, with increasing temperatures, the volume of ACFs increased initially, then decreased at the pore width of 0.5 to 1.0 nm, and then increased gradually at 1.0 to 2.0 nm and 2.0 to 10 nm. This suggested that the activation process not only generated new micropores, but also widened the existing pores (even to mesopores) by removing the active amorphous atoms and unsaturated carbon atoms from the edges of the micrographitic walls and partially gasifying the micropore walls (Ishii *et al*. 1997; Sánchez-Montero *et al*. 2008). This phenomenon can also be interpreted as the average pore diameter difference of ACFs (Table 1), ranging from 2.5 to 4.3 nm.

Surface Chemical Compositions

X-ray photoelectron spectroscopy (XPS) has been shown to be a useful tool for analyzing the surface groups of ACFs. The spectra of prepared ACFs are shown in Fig. 4(a). The major peaks in the spectra are attributed to C 1s and O 1s photoelectrons.

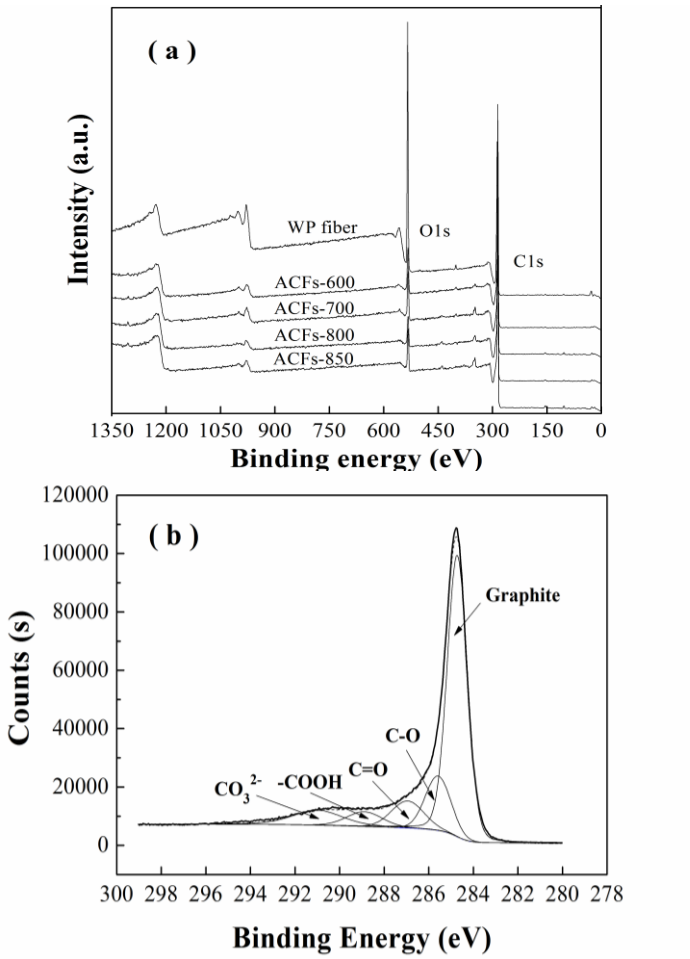

Fig. 4. X-ray photoelectron spectroscopy spectra of (a) ACFs and (b) C1s region for ACFs-800

Table 2 summarizes the elemental compositions on the surface of the samples. The contents of N, Si, and S atoms were quite low, and all of the samples were smaller than 2 at.% (atomic percent). Elemental carbon was the most abundant constituent in all of the samples, and the carbon content slightly increased with the increase in activation temperature, except at 850 °C. The violent reaction between carbon and steam at 850 °C may have resulted in only the partial conversion of micropores into mesopores. That is also why the oxygen content increased after the activation temperature was increased to 800 °C. These results are consistent with those determined by N_2 adsorption-desorption measurements (Table 1).

The C1s spectra for ACFs were very similar; therefore, only the spectrum for ACFs-800 is presented in Fig. 4(b), as an example. For all of the ACFs, the C 1s signals exhibited an asymmetric tailing, which was partially attributed to the intrinsic asymmetry of the graphite peaks or to the contribution of oxygen surface complexes. Deconvolution of the XPS C1s spectra produced five individual component peaks, representing graphitic carbon (284.6 to 284.7 eV), carbon present in alcohol, ether, or C=N groups (285.5 to 286.2 eV), carbonyl or quinine groups (286.9 to 287.1 eV), carboxyl, lactone, or ester groups (288.1 to 288.9 eV), and/or carbonate groups (290.7 eV) (Chiang *et al*. 2007).

Table 2. Elemental Composition of WP Fibers and Prepared ACFs Determined by XPS

Samples	C (at.%)	O (%)	N1 (%)	Si (%)	S (%)	O/C (%)	N/C (%)
ACFs-600	89.5	9.1	1.0	0.4	0.1	10.1	1.1
ACFs-700	88.6	9.0	0.6	1.7	0.0	10.2	0.7
ACFs-800	92.2	6.7	0.4	0.7	0.1	7.2	0.5
ACFs-850	89.4	8.8	0.5	1.2	0.1	9.8	0.5

Table 3 summarizes the percentages of graphitic and functional carbon atoms. The values in % intensity for graphitic carbon and oxygen-containing groups showed obvious differences among ACFs. After activation, the relative amount of the graphitic carbon in ACFs decreased as the temperature increased, whereas the C-O-containing functional groups changed in the opposite direction. In addition, the percentage of carbonate groups increased notably with increasing temperature. It is believed that more graphitic carbons of ACFs reacted with steam molecules to generate more functional groups containing C-O. The fact that more byproducts were released from ACFs in the form of CO_2, CO, or H_2O serves as a benefit in developing more pores and in damaging the graphitic structure, consistent with the analysis of the microstructure (Shen *et al*. 2011).

Table 3. Results of the Fits of the C1s Regions[a]

Samples	Graphite C–C (C_{P1})	C–OH (C_{P2})	C=O (C_{P3})	C–OOH (C_{P4})	CO_3^{2-}(C_{P5})
ACFs-600	62.8	20.1	8.1	5.1	3.9
ACFs-700	58.1	20.3	9.9	7.0	4.6
ACFs-800	57.1	19.5	9.8	7.5	6.2
ACFs-850	52.4	18.2	13.9	6.9	8.6
[a] Values given in % of total intensity					

FTIR Analysis

Fourier transform infrared spectroscopy (FTIR) provides an extremely useful method to investigate the functional groups. Figure 5 illustrates the FTIR spectra of WP fibers and ACFs prepared at various temperatures. The FTIR spectrum of WP fibers reveals a broad adsorption peak at 3412 cm^{-1}, attributed to the -OH vibration frequencies of hydroxyl groups (Silverstein *et al*. 2005). After carbonization and activation, higher intensities and broader signals were transformed into weaker signals, suggesting a decrease in the number of -OH groups present in the ACFs. Bands for C-H stretching of methyl and methylene groups (2912 cm^{-1}) almost disappeared in the FTIR spectra of ACFs. Bands from 1580 to 1640 cm^{-1} and 1690 to 1730 cm^{-1} correspond to conjugated C=O and unconjugated C=O stretching vibrations, respectively (Myglovets *et al*. 2014). The intensities of the C=O bands decreased and then increased with increasing activation temperature. Moreover, the intensity of adsorption peaks near 1119 cm^{-1}, assigned to C-O stretching vibration, increased, indicating the abundance of oxygen-containing functional groups within the ACFs. Therefore, the FTIR spectra of all ACFs showed less intense absorption bands than that of the WP fibers, revealing that the activation process with steam and heat facilitated the restructuring of the organic precursor of WP fibers into a carbon structure (Yacob *et al*. 2008). These results are also consistent with those of XPS.

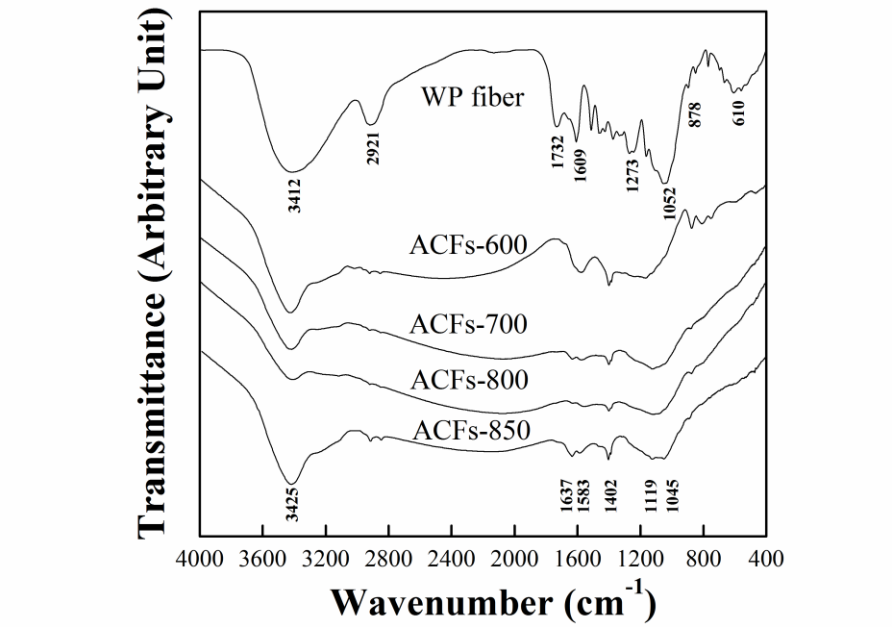

Fig. 5. Fourier transform infrared spectroscopy of WP fibers and of ACFs prepared by different activation temperatures

Adsorption of MB

ACFs showed high adsorption capacity for methylene blue with the rise of the activation temperature. The MB adsorption continued to increase as the temperature increased from 600 to 850 °C. When the temperature was 850 °C, the MB adsorption of ACFs reached 882 mg/g. The variations of MB adsorption for ACFs showed patterns similar to the V_{meso} values of N_2 adsorption mentioned above. The MB adsorption values of ACFs were also all much higher than those previously studies on the ACFs (20 to 626 mg/g) (Ma *et al*. 2014).

CONCLUSIONS

1. Renewable and highly available WP fibers (*Trachycarpus fortunei*) were successfully utilized as a precursor for the preparation of ACFs with steam activation temperatures ranging from 600 to 800 °C.
2. The ACFs with high surface area and total pore volume were obtained in this work, with the maximum value of 1320 m^2/g and 1.416 cm^3/g, respectively. The abundant porous structure, which were observed in the original windmill palm fibers, contributed to the generation of pores during the activation process.
3. New micropores were regenerated, and part of existing micropores were widened to mesopore structures during the activation process at 850 °C. However, the yield was very low in that case.
4. The obtained ACFs with high MB adsorption values in this study can be used as a very promising adsorbent for pollution control.

ACKNOWLEDGMENTS

The authors would like to thank the Fundamental Research Funds for the Central Universities (NO. BLX2014-42) for their financial support and the National Science & Technology Pillar Program during the Twelfth Five-Year Plan Period, Key Technology, and Application Demonstration for the Production of Wood-Based Functional Adsorption Materials (2015BAD14B06).

REFERENCES CITED

Chen, S., and Zeng, H. (2003). "Improvement of the reduction capacity of activated carbon fiber," *Carbon* 41(6), 1265-1271. DOI: 10.1016/S0008-6223(03)00077-0

Chiang, Y., Lee, C., and Lee, H. (2007). "Characterization of microstructure and surface properties of heat-treated PAN-and rayon-based activated carbon fibers," *J. Porous Mater*. 14(2), 227-237. DOI: 10.1007/s10934-006-9028-8

Ishii, C., Suzuki, T., Shindo, N., and Kaneko, K. (1997). "Structural characterization of heat-treated activated carbon fibers," *J. Porous Mater*. 4(3), 181-186. DOI: 10.1023/A: 1009614901091

Jain, A., Balasubramanian, R., Srinivasan, M. P. (2016). "Hydrothermal conversion of biomass waste to activated carbon with high porosity: A review," *Chem. Eng. J*. 283, 789-805. DOI: 10.1016/j.cej.2015.08.014

Jin, Z., and Zhao, G. (2014). "Porosity evolution of activated carbon fiber prepared from liquefied wood. Part I: water steam activation at 650 to 800 °C," *BioResources* 9(2), 2237-2247. DOI: 10.15376/biores.9.2.2237-2247

Lastoskie, C., Gubbins, K. E., and Quirke, N. (1993). "Pore size distribution analysis of microporous carbon: A density functional theory approach," *J. Phys. Chem.* 97(18), 4786-4796. DOI: 10.1021/j100120a035

Lee, T., Ooi, C., Othman, R., Yeoh, F. (2014). "Activated carbon fiber - The hybrid of carbon fiber and activated carbon," *Rev. Adv. Mater. Sci.* 36(2), 118-136.

Leon, C. A. L. Y. (1998). "New perspectives in mercury porosimetry," *Adv. Colloid Interf. Sci*. 76-77, 341-372. DOI: 10.1016/S0001-8686(98)00052-9

Li, J., Ng, D. H. L., Song, P., Kong, C., Song, Y., and Yang, P. (2015). "Preparation and characterization of high-surface-area activated carbon fibers from silkworm cocoon waste for congo red adsorption," *Biomass Bioenerg.* 75, 189-200. DOI: 10.1016/j.biombioe.2015.02.002

Liu, W. J., and Zhao, G. J. (2012). "Effect of temperature and time on microstructure and surface functional groups of activated carbon fibers prepared from liquefied wood," *BioResources* 7(4), 5552-5567. DOI: 10.15376/biores.7.4.5552-5567

Liu, W. J., Shi, M. R., Ma, E. N., and Zhao, G. J. (2014). "Microstructure and properties of liquefied wood based activated carbon fibers prepared from precursors and carbon fiber," *Wood Fiber Sci.* 46(1), 39-47.

Ma, X. J., Yang, H. M., Yu, L. L., Chen, Y., and Li, Y. (2014). "Preparation, surface and pore structure of high surface area activated carbon fibers from bamboo by steam activation," *Materials* 7(6): 4431-4441. DOI: 10.3390/ma7064431

Myglovets, M., Poddubnaya, O. I., Sevastyanova, O., Lindstrom, M. E., Gawdzik, B., Sobiesiak, M., Tsyba, M. M., Sapsay, V. I., Klymchuk, D. O., and Puziy, A. M. (2014). "Preparation of carbon adsorbents from lignosulfonate by phosphoric acid activation for the adsorption of metal ions," *Carbon* 80, 771-783. DOI: 10.1016/j.carbon.2014.09.032

Qian, Q., Machida, M., and Tatsumoto, H. (2007). "Preparation of activated carbons from cattle-manure compost by zinc chloride activation," *Bioresour. Technol.* 98(2), 353-360. DOI: 10.1016/j.biortech.2005.12.023

Rosas, J. M., Bedia, J., Rodríguez-Mirasol, J., and Cordero, T. (2009). "Hemp-derived activated carbon fibers by chemical activation with phosphoric acid," *Fuel* 88(1), 19-26. DOI: 10.1016/j.fuel.2008.08.004

Sánchez-Montero, M. J., Salvador, F., and Izquierdo, C. (2008). "Reactivity and porosity of a carbon fiber activated with supercritical CO_2," *J. Phys. Chem. C* 112(13), 4991-4999. DOI: 10.1021/jp709647y

Shen, Q., Zhang, T., Zhang, W., Chen, S., and Mezgebe, M. (2011). "Lignin-based activated carbon fibers and controllable pore size and properties," *J. Appl. Polym. Sci*. 121(2), 989-994. DOI: 10.1002/app.33701

Silverstein, R. M., Webster, F. X., and Kiemle, D. J. (2005). "Infrared spectroscopy," in: *Spectrometric Identification of Organic Compounds*, M. S. Robert (ed.), Wiley, Hoboken, NJ, pp 72-108.

Sing, K. S. W., Everett, D. H., Haul, R. A. W., Moscou, L., Pierotti, R. A., Rouquerol, J., and Siemieniewska, T. (1985). "Reporting physisorption data for gas/solid systems with special reference to the determination of surface area and porosity," *Pure Appl. Chem.* 57(4), 603-619. DOI: 10.1351/pac198557040603

Su, C., Zeng, Z., Peng, C., and Lu, C. (2012). "Effect of temperature and activators on the characteristics of activated carbon fibers prepared from viscose-rayon knitted fabrics," *Fiber Polym.* 13(1), 21-27. DOI: 10.1007/s12221-012-0021-3

Suhas, P. J. M. C., and Carrott, M. M. L. R. (2007). "Lignin-from natural adsorbent to activated carbon: A review," *Bioresour. Technol*. 98(12), 2301-2312. DOI: 10.1016/j.biortech.2006.08.008

Suzuki, M. (1994). "Activated carbon fiber: Fundamentals and applications," *Carbon* 32(4), 577-586. DOI: 10.1016/0008-6223(94)90075-2

Wigmans, T. (1989). "Industrial aspects of production and use of activated carbons," *Carbon* 27(1), 13-22. DOI: 10.1016/0008-6223(89)90152-8

Wu, F. C., Tseng, R. L., and Juang, R. S. (1999a). "Pore structure and adsorption performance of the activated carbons prepared from plum kernels," *J. Hazard. Mater*. 69(3), 287-302. DOI: 10.1016/S0304-3894(99)00116-8

Wu, F. C., Tseng, R. L., and Juang, R. S. (1999b). "Preparation of activated carbons from bamboo and their adsorption abilities for dyes and phenol," *J. Environ. Sci. Health A* 34(9), 1753-1775. DOI: 10.1080/10934529909376927

Yang, R., Liu, G., Xu, X., Li, M., Zhang, J., and Hao, X. (2011). "Surface texture, chemistry and adsorption properties of acid blue 9 of hemp (*Cannabis sativa L*.) bast-based activated carbon fibers prepared by phosphoric acid activation," *Biomass Bioenerg.* 35(1), 437-445. DOI: 10.1016/j.biombioe.2010.08.061

Yacob, A. R., Majid, Z. A., Dasril, R. S. D., and Inderan, V. (2008). "Comparison of various sources of high surface area carbon prepared by different types of activation," *Malaysian J. Anal. Sci*. 12(1), 264-271.

Zabaniotou, A., Stavropoulos, G., and Sloulou, V. (2008). "Activated carbon from olive kernels in a two-storage process: Industrial improvement," *Bioresour. Technol*. 99(2), 320-326. DOI: 10.1016/j.biortech.2006.12.020

Zhai, S., Li, D., Pan, B., Sugiyama, J., and Itoh, T. (2012). "Tensile strength of windmill palm (*Trachycarpus fortunei*) fiber bundles and its structural implications," *J. Mater. Sci*. 47(2), 949-959. DOI: 10.1007/s10853-011-5874-0

Zhai, S., Horikawa, Y., Imai, T., and Sugiyama, J. (2013). "Cell wall characterization of windmill palm (*Trachycarpus fortunei*) fibers and its functional implications," *IAWA J*. 34(1), 20-33. DOI: 10.1163/22941932-00000003

Zhang, C. L., Zhang, J., Zou, H. Y., Shi, Q. Q., Li, Y., and Wang, L. (2008). "Method for producing windmill palm tegument activated carbon fiber with biological-chemical method," China Patent NO. CN101245501A, issued August 20, 2008.

Zhao, Y., Fang, F., Xiao, H., Feng, Q., Xiong, L., and Fu, S. (2015). "Preparation of pore-size controllable activated carbon fibers from bamboo fibers with superior performance for xenon storage," *Chem. Eng. J*. 270, 528-534. DOI: 10.1016/j.cej.2015.02.054

Zheng, J. Y., Zhao, Q. L., and Ye, Z. F. (2014). "Preparation and characterization of activated carbon fiber (ACF) from cotton woven waste," *Appl. Surf. Sci*. 299, 86-91. DOI: 10.1016/j.apsusc.2014.01.190

Article submitted: September 9, 2015; Peer review completed: November 7, 2015; Revised version received and accepted; December 6, 2015; Published: December 18, 2015.
DOI: 10.15376/biores.11.1.1596-1608